Chemical Engineering Journal 144 (2008) 407–419

Contents lists available at ScienceDirect

Chemical Engineering Journal

journal homepage: www.elsevier.com/locate/cej

Start-up of a nitrification system with automatic control to treat highly concentrated ammonium wastewater: Experimental results and modeling

Irene Jubany, Julián Carrera*, Javier Lafuente, Juan A. Baeza

Department of Chemical Engineering, Escola Tècnica Superior d'Enginyeria (ETSE), Universitat Autònoma de Barcelona, Spain

ARTICLE INFO

Article history:
Received 3 October 2007
Received in revised form 4 February 2008
Accepted 14 February 2008

Keywords:
Nitrification
Start-up
Control
Modeling
OUR

ABSTRACT

The start-up of a biological nitrifying system to treat high-strength ammonium wastewater must be done carefully to avoid ammonium or nitrite build-up and subsequent system destabilization due to inhibition. This article shows the start-up with automatic control of a complete nitrification system in a pilot plant. Firstly, a manual start-up was performed with manual increases in the nitrogen-loading rate (NLR). Secondly, two control strategies for controlled start-up based on oxygen uptake rate (OUR) measurements were successfully implemented and compared in the pilot plant. The successful enrichment of the microbial community in nitrifying microorganisms was corroborated with fluorescence in situ hybridization (FISH) quantification. Finally, the results of both controlled start-up strategies were simulated with a mathematical model considering the nitrification as a two-step process.

1. Introduction

The start-up of a biological process always requires special attention. If the start-up strategy is not appropriate, loss of biomass or destabilization of the process can easily occur [1]. Start-up of an activated sludge system usually consists of a progressively enrichment of the microbial community in a specific group of microorganisms (nitrifiers, polyphosphate accumulating organisms (PAOs), heterotrophs, etc.). Usually, the growing conditions of the inoculum are gradually changed until the desired conditions are reached. These conditions could be the temperature, contaminant load, shear stress, etc. Therefore, a successful start-up is accomplished when the inoculated population is enriched in the target population or acclimated to the final conditions. For example, an activated sludge reactor for biological denitrification reached the steady state 80–100 d after the inoculation with fresh sludge from a wastewater treatment plant (WWTP), but only 25–30 d after inoculation when acclimated sludge was used as seeding [2].

One of the most problematic steps in the biological nitrogen removal (BNR) process of high-strength ammonium wastewaters, for instance the reject water from the dewatering system of digested sludge, is the start-up of the nitrifying process. Ammonium accumulation, due to disturbances as changes in temperature, inflow or dissolved oxygen concentration, can provoke the inhibition of nitrification and consequently the BNR instability. Reported experiences for the start-up procedure for highly nitrogenous wastewaters show that it is quite delicate and time-consuming (3–4 months [3] or around 100 d [4]). During this operation a large accumulation of ammonium can take place if the nitrogen-loading rate (NLR) is higher than the maximum nitrification rate (MNR) of the system. Therefore, the start-up must be carried out with a gradual and controlled increase of the NLR, so that the nitrification rate is as close as possible to the MNR [5].

The start-up of a nitrifying process is usually carried out with manual control based on total ammonia nitrogen (TAN), total nitrite nitrogen (TNN), nitrate or oxygen uptake rate (OUR) measurements [4–7]. In these studies, nitrogenous compounds or OUR, in the effluent or in the aerobic reactor, were measured and the NLR was manually changed accordingly: increased if the percentage of nitrification was satisfactory or decreased if the undesirable compounds were building up. Each NLR was maintained for some days (2–10 d) before a new NLR was applied. The NLR was changed by either increasing inflow or concentration, depending on whether constant hydraulic retention time (HRT) was required. In some studies, a combination of both options was used [8].

Automatic control has been widely applied to improve nitrogen removal in WWTPs with online TAN analyzers [9,10]. Other researchers preferred in-line measurements as pH, oxido-reduction potential (ORP) and dissolved oxygen (DO) because the complexity of measuring the chemical compounds in real-time is neither simple nor economical [11,12]. Although automatic control is still being studied and applied in pilot plant and full-scale systems to improve nutrients removal, there is a lack of studies to improve the start-up process with automatic control strategies.

The objectives of this work are: (1) to implement and test two control strategies for the start-up of a nitrifying system from a

* Corresponding author.
E-mail address: julian.carrera@uab.es (J. Carrera).

1385-8947/$ – see front matter © 2008 Elsevier B.V. All rights reserved.
doi:10.1016/j.cej.2008.02.010

Nomenclature

AOB	ammonia oxidising bacteria
BNR	biological nitrogen removal
DO	dissolved oxygen
FA	free ammonia
F_{ER}	flow external recycle
F_{IR}	flow internal recycle
FISH	fluorescence in situ hybridization
FNA	free nitrous acid
HRT	hydraulic retention time
MNR	maximum nitrification rate
NLR	nitrogen-loading rate
NLR_S	specific nitrogen-loading rate
NOB	nitrite oxidising bacteria
OLR	organic-loading rate
OUR	oxygen uptake rate
OUR_{NOB}^{max}	maximum OUR due to nitratation
OUR_{end}	endogenous oxygen uptake rate
OUR_{sp}	oxygen uptake rate set point
S_{TAN}	total ammonia nitrogen
S_{TNN}	total nitrite nitrogen
S_{NO_3}	nitrate
S_{ND}	soluble biodegradable organic nitrogen
S_O	dissolved oxygen
S_S	readily biodegradable organic matter
SRT	sludge retention time
SVI	sludge volumetric index
TAN	total ammonia nitrogen
TNN	total nitrite nitrogen
TSS	total suspended solids
VSS	volatile suspended solids
X_A	ammonia oxidising bacteria
X_N	nitrite oxidising bacteria
X_H	heterotrophic bacteria
X_P	inert products
X_S	slowly biodegradable organic matter
X_N	particulate biodegradable organic nitrogen

mainly heterotrophic sludge for treating high-strength ammonium wastewater, for instance reject water from dewatering system of digested sludge. These control strategies will be based on OUR measurements. (2) To check the validity of the mathematical model to predict the experimental results of the start-ups with automatic control. (3) To use the model to predict the behavior of the system in the long term.

2. Materials and methods

This section includes the description of the experimental conditions and the inoculum characteristics for the three start-up experiments carried out in this work: a manual start-up (I) and two automatically controlled start-ups (II and III). The experimental inflow control loop is also shown and some details are pointed out with respect to modeling and chemical analyses.

2.1. Pilot plant

The start-up experiments (start-ups I, II and III) were performed in a pilot plant that consisted of three aerobic reactors (named R1, R2 and R3) with a working volume of 26 L followed by a 25 L settler (Fig. 1). The reactors were connected in series and they worked under completely mixed conditions. A fraction of R3 effluent was

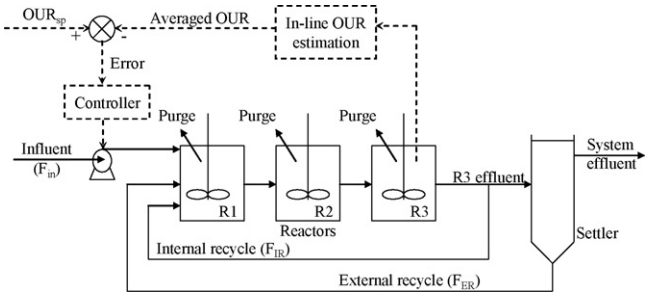

Fig. 1. Diagram of the inflow control loop in the pilot plant with OUR as the measured variable.

recycled to R1 (internal recycle) to increase the dynamics of the system and to improve the mixing between reactors. Mixed liquor was withdrawn daily from the three reactors in order to keep a desired sludge retention time (SRT). Each reactor was equipped with DO (WTW Oxi 340i CellOx 325), pH (Crison pH 52-03) and temperature probes. They were connected to probe controller equipment (Crison pHrocon18) which actuated as a pH on–off controller in R1 and R2 by the addition of solid sodium carbonate through solid dispensers. The probe controller equipment was connected to a process computer which was in charge of control of the key process parameters (DO, temperature, flow-rates and stirring rates). The DO control was based on a digital proportional–integral–derivative (PID) manipulating pneumatic control valves which modified the airflow supplied through air diffusers placed at the bottom of the reactors. The on–off temperature control was implemented operating on an electric heating device.

Automatic in-line OUR estimation was implemented in each reactor. The OUR measurement was performed every 5 or 10 min and it was based on the DO decrease in the liquid phase with no air inlet. The OUR measurement followed these steps: deactivation of the DO PID controller, aeration valve shut down, DO measurement every 4 s until it decreased by 1.5 mg O_2 L^{-1} and calculation of OUR with the slope of acquired data. A more detailed description of the pilot plant, control system and OUR estimation can be found elsewhere [10,13].

The influent consisted of synthetic wastewater with high ammonium concentration (3000 mg N L^{-1}) and low biodegradable COD concentration (100 mg COD L^{-1}). Micronutrients were also supplied [13].

The experimental conditions in the three start-ups were slightly different among them since the system performance was being improved as the experiments were being performed. The main differences were the temperature control, implemented in R2 when start-up III was performed, and the in-line OUR estimation which was implemented in all reactors after start-up I (Table 1).

Sludges from two municipal WWTPs from the area of Barcelona were used to inoculate the pilot plant for the different start-up experiments. These WWTPs were performing nitrification at the time of biomass collection but their nitrogen removal rates were very low since the applied NLR was low (0.013–0.05 g N g^{-1} VSS d^{-1}). This means that the fraction of nitrifying bacteria was also low in the seeded sludges.

2.2. Off-line respirometric experiments

Off-line respirometric tests were performed off-line with the respirometer described by Jubany [14]. Each of the estimations of the MNR in start-up I was carried out by adding a TAN pulse of 40 mg N L^{-1} (non-limiting concentration) into the respirometer and measuring the DO drop in triplicate. Temperature, pH and DO were kept equal to measurements in the pilot plant. Estimated OUR was

Table 1
Experimental conditions in the pilot plant in each start-up experiment

Experiment	pH	T	DO	OUR estimation
Start-up I	Controlled in R1 and R2 at 7.5	Not controlled	Controlled in each reactor at 3.0 mg O_2 L^{-1}	Manual off-line every week
Start-up II	Controlled in R1 and R2 at 7.5	Not controlled	Controlled in each reactor at 3.0 mg O_2 L^{-1}	Automatic in-line every 15 min
Start-up III	Controlled in R1 and R2 at 7.5	Controlled in R2	Controlled in each reactor at 3.0 mg O_2 L^{-1}	Automatic in-line every 5 min

corrected with the endogenous OUR and the MNR was calculated as shown in Eq. (1),

$$\mathrm{MNR} = \frac{\mathrm{OUR}}{[\mathrm{VSS}] \cdot (4.57 - Y_A - Y_N)} \quad (1)$$

where [VSS] is the VSS concentration, 4.57 is the stoichiometric coefficient for oxygen in the global nitrification process and Y_A and Y_N are the growth yield coefficients for ammonia oxidising bacteria (AOB) and nitrite oxidising bacteria (NOB), respectively.

2.3. Experimental inflow control loop

In start-up II and III, an inflow control loop was implemented in a supervisory expert control system developed in G2©(version 4.1), running in a Sun workstation. This expert system had already been developed and applied in the same pilot plant [10]. The control loop consisted of a feedback controller where the measured variable was the OUR in R3. Every 10 min, the supervisory expert controller calculated an averaged OUR value with values from the last 30 min and compared it with the OUR set point ($\mathrm{OUR_{sp}}$). The difference among these two OUR values was used, together with the controller algorithm, to calculate a new inflow value. Finally, the control action was transmitted to the process computer that changed the pulse frequency of the inflow pumps. The controller algorithms were an on–off controller in start-up II and a proportional–integral (PI) controller in start-up III. These algorithms were designed and optimized by means of simulation tools in a previous article [15]. The controllers parameters used were adapted from the previous work: on–off controller with automatic inflow increases of 30% for start-up II and $Kc = 0.002\,(L\,d^{-1})\,(mg\,O_2\,L^{-1}\,d^{-1})^{-1}$ and $\tau_I = 0.142$ d for start-up III. For a more detailed explanation of the controller algorithms see Jubany et al. [15]. Fig. 1 schematically shows the control loop implemented in the pilot plant.

2.4. Analyses and FISH

TAN was analyzed by means of a continuous flow analyzer (CFA) based on potentiometric determination of ammonia [16]. TNN and nitrate were measured with capillary electrophoresis using a WATERS Quanta 4000E CE according to Carrera et al. [5]. Volatile suspended solids (VSS), total suspended solids (TSS) and sludge volumetric index (SVI) were determined according to standard methods [17].

Fluorescence in situ hybridization (FISH) technique coupled with confocal microscopy was used to determine the predominant nitrifying species during start-up III. A Leica TCS SP2 AOBS confocal laser scanning microscope (CLSM) at a magnification of ×63 (objective HCX PL APO ibd.B1 63 × 1.4 oil) equipped with two HeNe lasers with light emission at 561 and 633 nm was used for biomass quantification. Hybridizations were carried out using at the same time a Cy3-labeled specific probe and Cy5-labeled EUB-mix probes. Specific probe used for AOB detection was Nso190 and for NOB detection were Ntspa662 and NIT3. Detailed information about FISH quantification method can be found in Jubany [14].

2.5. Model development and description

Nitrification was modelled as a two-step process which considered AOB and NOB populations. Heterotrophic bacteria were also included to be able to describe the total biomass concentration since it has been shown that enriched nitrifying systems have a relatively high content of heterotrophic bacteria [18,19] and furthermore, the influent of the real system contained some COD. Six soluble compounds were considered (as concentration in the bulk liquid): total ammonia nitrogen (S_{TAN}), total nitrite nitrogen (S_{TNN}), nitrate (S_{NO_3}), soluble biodegradable organic nitrogen (S_{ND}), dissolved oxygen (S_O) and readily biodegradable organic matter (S_S). Inorganic carbon concentration (CO_2 or HCO_3^-) was not considered because it was always in excess due to the pH control with sodium carbonate and therefore it never limited the biomass growth. With respect to the particulate compounds, AOB (X_A), NOB (X_N), heterotrophic bacteria (X_H), inert products arising from biomass decay (X_P), slowly biodegradable organic matter (X_S) and particulate biodegradable organic nitrogen (X_{ND}) were considered.

The terms TAN ($N\text{-}NH_4^+ + N\text{-}NH_3$) and TNN ($N\text{-}NO_2^- + N\text{-}HNO_2$) were used instead of ammonium and nitrite because they are the true compounds analyzed in the chemical analyses. Eqs. (2) and (3), derived from acid–base equilibriums, were used for the calculation of the free ammonia (FA or NH_3) and the free nitrous acid (FNA or HNO_2) concentrations in equilibrium with TAN and TNN, respectively.

$$\mathrm{FA} = \frac{\mathrm{TAN} \cdot 10^{\mathrm{pH}}}{(K_b/K_w) + 10^{\mathrm{pH}}} \cdot \frac{17}{14} \quad (2)$$

$$\mathrm{FNA} = \frac{\mathrm{TNN}}{K_a \cdot 10^{\mathrm{pH}} + 1} \cdot \frac{47}{14} \quad (3)$$

Table 2
Process kinetics for the two-step nitrification model including heterotrophic bacteria

Process	Process rate (d^{-1})
1. Growth of X_A	$\mu_{max,A} \cdot \frac{S_O}{K_{O,A}+S_O} \cdot \frac{S_{TAN}}{K_{S,TAN,A}+S_{TAN}+(S_{TAN}^2/K_{I,TAN,A})} \cdot \frac{K_{I,TNN,A}}{K_{I,TNN,A}+S_{TNN}} \cdot X_A$
2. Growth of X_N	$\mu_{max,N} \cdot \frac{S_O}{K_{O,N}+S_O} \cdot \frac{S_{TNN}}{K_{S,TNN,N}+S_{TNN}+(S_{TNN}^2/K_{I,TNN,N})} \cdot \frac{K_{I,TAN,N}}{K_{I,TAN,N}+S_{TAN}} \cdot X_N$
3. Growth of X_H	$\mu_{max,H} \cdot \frac{S_O}{K_{O,H}+S_O} \cdot \frac{S_S}{K_{S,H}+S_S} \cdot X_H$
4. Decay of X_A	$b_A \cdot X_A$
5. Decay of X_N	$b_N \cdot X_N$
6. Decay of X_H	$b_H \cdot X_H$
7. Ammonification of S_{ND}	$k_a \cdot S_{ND} \cdot X_H$
8. Hydrolysis of X_S	$k_h \cdot \frac{X_S/X_H}{K_X+X_S/X_H} \cdot \frac{S_O}{K_{O,H}+S_O} \cdot X_H$
9. Hydrolysis of X_{ND}	$k_h \cdot \frac{X_S/X_H}{K_X+X_S/X_H} \cdot \frac{S_O}{K_{O,H}+S_O} \cdot X_H \cdot \frac{X_{ND}}{X_S}$

The ratio between the ionization constant of the ammonia equilibrium (K_b) and the ionization constant of water (K_w) is related to the temperature as shown in Eq. (4), and the temperature effect on the ionization constant of the nitrous acid equilibrium (K_a) is shown in Eq. (5) [20].

$$\frac{K_b}{K_w} = \exp\left(\frac{6344}{273+T}\right) \quad (4)$$

$$K_a = \exp\left(\frac{-2300}{273+T}\right) \quad (5)$$

Table 2 shows the kinetics for each of the processes considered: growth and decay of each kind of bacteria, ammonification of soluble organic nitrogen, hydrolysis of entrapped organics and hydrolysis of entrapped organic nitrogen. Also, the oxygen limitations, substrate and non-competitive inhibitions for AOB and NOB growth processes were considered. AOB inhibition by TAN and NOB inhibition by TNN were described with a Haldane model while AOB inhibition by TNN and NOB inhibition by TAN were described with a non-competitive model. The stoichiometry of the processes is shown in Table 3.

It is quite accepted that FA and FNA are the preferred substrates of AOB and NOB, respectively, and also the inhibitory species [20]. If these statements are taken into account, the affinity constants for substrate and the inhibition coefficients used in this model should be considered constants in terms of FA and FNA and dependent on pH and temperature in terms of TAN and TNN. Therefore, Eqs. (2)–(5) were included in the model.

Table 4 summarizes all the model parameters required to describe the nitrification as a two-step process considering also heterotrophic bacteria. Parameters dependent on pH and temperature (maximum specific growth rates and decay rates) were calculated at 25 °C and a pH of 7.5. The expressions to calculate them under other conditions are shown in Eqs. (6)–(11) [14].

$$\mu_{max,A}(pH,T) = \frac{1.28\times10^{12}\cdot\exp(-8183/(273+T))}{1+((2.05\times10^{-9})/10^{-pH})+(10^{-pH}/(1.66\times10^{-7}))} \quad (6)$$

$$b_A(T) = 1.651\times10^{11}\cdot\exp\left(\frac{-8183}{273+T}\right) \quad (7)$$

$$\mu_{max,N}(pH,T) = \frac{6.69\times10^{7}\cdot\exp(-5295/(273+T))}{1+((2.05\times10^{-9})/10^{-pH})+(10^{-pH}/(1.66\times10^{-7}))} \quad (8)$$

$$b_N(T) = 8.626\times10^{6}\cdot\exp\left(\frac{-5295}{273+T}\right) \quad (9)$$

$$\mu_{max,H} = 6\cdot(1.07)^{(T-20)} \quad (10)$$

$$b_H = 0.4\cdot(1.07)^{(T-20)} \quad (11)$$

where the equations are expressed in terms of d^{-1} and the temperature is in °C.

All simulations were performed with Matlab 6.5® [22]. The ode15 s function, a variable order solver based on the numerical differentiation formulas, was used to solve the differential equations of the model.

3. Results and discussion

3.1. Experimental start-up without automatic control (start-up I)

The first start-up experiment was done with manual increases of the NLR. This experiment was used as a reference for the start-up experiments with automatic inflow control. Inoculated

Table 3
Process stoichiometry for the two-step nitrification model including heterotrophic bacteria

Process	Compounds												
	S_{TAN} ($mg\,N\,L^{-1}$)	S_{TNN} ($mg\,N\,L^{-1}$)	S_{NO_3} ($mg\,N\,L^{-1}$)	S_{ND} ($mg\,N\,L^{-1}$)	S_O ($mg\,O_2\,L^{-1}$)	S_S ($mg\,COD\,L^{-1}$)	X_A ($mg\,COD\,L^{-1}$)	X_N ($mg\,COD\,L^{-1}$)	X_H ($mg\,COD\,L^{-1}$)	X_P ($mg\,COD\,L^{-1}$)	X_S ($mg\,COD\,L^{-1}$)	X_{ND} ($mg\,N\,L^{-1}$)
1. Growth of X_A	$-(1/Y_A)-i_{XB}$	$1/Y_A$	0	0	$-(3.43-Y_A)/(Y_A)$	0	1	0	0	0	0	0
2. Growth of X_N	$-i_{XB}$	$-(1/Y_N)$	$1/Y_N$	0	$-(1.14-Y_N)/(Y_N)$	0	0	1	0	0	0	0
3. Growth of X_H	$-i_{XB}$	0	0	0	$-(1-Y_A)/(Y_A)$	$-(1/Y_H)$	0	0	1	0	0	0
4. Decay of X_A	0	0	0	0	0	0	−1	0	0	f_P	$1-f_P$	$i_{XB}-f_P\cdot i_{XP}$
5. Decay of X_N	0	0	0	0	0	0	0	−1	0	f_P	$1-f_P$	$i_{XB}-f_P\cdot i_{XP}$
6. Decay of X_H	0	0	0	0	0	0	0	0	−1	f_P	$1-f_P$	$i_{XB}-f_P\cdot i_{XP}$
7 Ammonification of S_{ND}	1	0	0	−1	0	0	0	0	0	0	0	0
8. Hydrolysis of X_S	0	0	0	0	0	1	0	0	0	0	−1	0
9. Hydrolysis of X_{ND}	0	0	0	1	0	0	0	0	0	0	0	−1

Table 4
Stoichiometric and kinetic parameters for the two-step nitrification model including heterotrophic bacteria at $T = 25\,^{\circ}C$ and pH 7.5

Name	Units	Symbol	Value	Reference
Parameters related to AOB				
Growth yield	g COD g^{-1} N	Y_A	0.18	[14]
Maximum specific growth rate	d^{-1}	$\mu_{max,A}$	1.21	[14]
Decay rate	d^{-1}	b_A	0.20	[14]
Affinity constant for DO	mg O_2 L^{-1}	$K_{O,A}$	0.74	[14]
Affinity constant for FA	mg FA L^{-1}	$K_{S,FA,A}$	0.24	[14]
Inhibition coefficient for FA	mg FA L^{-1}	$K_{I,FA,A}$	7.0	[14]
Inhibition coefficient for FNA	mg FNA L^{-1}	$K_{I,FNA,A}$	0.55	[14]
Parameters related to NOB				
Growth yield	g COD g^{-1} N	Y_N	0.08	[14]
Maximum specific growth rate	d^{-1}	$\mu_{max,N}$	1.02	[13]
Decay rate	d^{-1}	b_N	0.17	[13]
Affinity constant for DO	mg O_2 L^{-1}	$K_{O,N}$	1.75	[14]
Affinity constant for FNA	mg FNA L^{-1}	$K_{S,FNA,N}$	4×10^{-4}	[14]
Inhibition coefficient for FNA	mg FNA L^{-1}	$K_{I,FNA,N}$	0.06	[14]
Inhibition coefficient for FA	mg FA L^{-1}	$K_{I,FA,N}$	0.95	[14]
Parameters related to heterotrophs				
Growth yield	g COD g^{-1} COD	Y_H	0.67	[21]
Maximum specific growth rate	d^{-1}	$\mu_{max,H}$	8.42	[21]
Decay rate	d^{-1}	b_H	0.56	[21]
Affinity constant for S_{O2}	mg O_2 L^{-1}	$K_{O,H}$	0.2	[21]
Affinity constant for S_S	mg COD L^{-1}	K_S	4	[21]
Other parameters				
Nitrogen content of X_A, X_N, X_H	g N g^{-1} COD	i_{XB}	0.08	[14]
Nitrogen content of X_P	g N g^{-1} COD	i_{XP}	0.06	[21]
Fraction of biomass leading X_P	g COD g^{-1} COD	f_P	0.08	[21]
Ammonification rate	L mg^{-1} COD d^{-1}	k_a	0.08	[21]
Maximum specific hydrolysis rate	g COD g^{-1} COD d^{-1}	k_h	3.0	[21]
Affinity constant for X_S	g COD g^{-1} COD	K_X	0.03	[21]

biomass was withdrawn from the WWTP of Centelles (Barcelona). Operational conditions during the whole experiment are described in Table 5.

At the beginning, the specific NLR (NLR_s) was fixed at the same value as it was in the full-scale plant (0.013 g N g^{-1} VSS d^{-1}). The aim of the start-up was to change the biomass composition from basically heterotrophic to mainly nitrifying. It was decided that TAN and TNN concentration in the effluent had to remain below 10 mg N L^{-1} in all the start-up. Therefore, the NLR_s had to be always below the MNR. The key point was to decide the best strategy to progressively increase the NLR_s avoiding TAN or TNN accumulation in the effluent. The strategy was to periodically measure the MNR with off-line OUR measurements and change the NLR_s accordingly. NLR_s was increased by raising both inflow value (from 15 to 30 L d^{-1}) and the feed concentration (from 100 to 1000 mg N-TAN L^{-1}). Fig. 2a shows the evolution of both NLR_s and MNR. It also shows the decrease in the ratio between MNR and NLR_s from a very conservative value (8) to a more optimal one (2) since the objective was to operate with NLR_s close to the MNR. TAN and TNN concentrations remained close to zero during all the experiment.

Fig. 2b shows the evolution of the biomass concentration which decreased dramatically from 3500 to 600 mg VSS L^{-1}. This was due to the decay of heterotrophic bacteria because the organic-loading rate (OLR) in the pilot plant through the experiment was approximately 50 times lower than in the municipal WWTP. This figure also shows that the SVI was lower than 150 mL g^{-1} which indicated, together with the fact that the TSS in the effluent were around 60 ± 15 mg TSS L^{-1}, that the settling properties of the sludge were good.

At the end of this start-up (day 96) a nitrifying sludge capable of treating a NLR_s of 0.4 g N g^{-1} VSS d^{-1} (or volumetric NLR: $NLR_v = 0.24$ g N L^{-1} d^{-1}) was obtained even though the reached biomass concentration was quite low (600 mg VSS L^{-1}). The achieved NLR_s was used as a reference value for the following start-ups with automatic control. This NLR_s was considered the target NLR_s because in Carrera et al. [5] the MNR achieved with a similar system was 0.37 g N g^{-1} VSS d^{-1} at 25 °C. A similar start-up was carried out in Ghyoot et al. [7] with a membrane-assisted bioreactor to remove nitrogen from sludge reject water. The strategy was also to conduct OUR measurements for the determination of the nitrifying capacity of the activated sludge and then adjust the NLR accordingly. In their work, the MNR/NLR_s was kept always close to one and as a consequence, any perturbation caused TAN and TNN accumulation which was not desired. It represents a good example of how difficult it is to manually start up a nitrifying system if MNR is wanted.

3.2. Experimental start-up with automatic on–off control (start-up II)

Operational conditions for start-up II are described in Table 5. The pilot plant was inoculated with biomass from the municipal

Table 5
Operational conditions in the pilot plant during the three start-ups (F_{IR} is the internal recycle flow and F_{ER} is the external recycle flow)

Start-up	pH	T (°C)	DO (mg O_2 L^{-1})	SRT (d)	F_{IR} (L d^{-1})	F_{ER} (L d^{-1})
I	7.5 ± 0.3	23 ± 2	3.5 ± 0.2	25	300	88
II	7.7 ± 0.3	23 ± 2	3.0 ± 0.2	15	330	29
III	7.6 ± 0.3	R1: 22 ± 2 R2: 27 ± 4 R3: 25 ± 3	3.0 ± 0.2	15	346	22

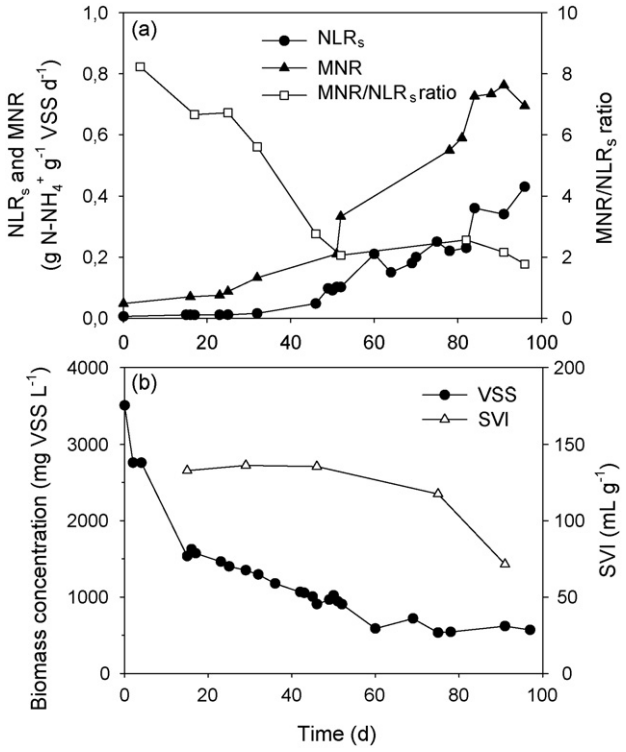

Fig. 2. Start-up I. (a) NLRs, MNR and ratio between them and (b) VSS and SVI.

WWTP of Centelles (Barcelona) and immediately fed with similar NLR_s than the one in the full-scale plant but 50 times lower OLR. TAN and COD concentrations in the influent were 2800 mg N L^{-1} and 100 mg COD L^{-1}, respectively, in the entire experiment, thus NLR_s was changed by changing only the inflow.

The on–off controller stopped the feeding pump when the OUR in R3 was higher than the OUR_{sp} and the inflow was set to a fixed value when the OUR in R3 was lower than the OUR_{sp}. The inflow value for the on-control action was successively increased in a 30% when the actual inflow value did not cause ammonium and nitrite accumulation in the effluent of R3 during several hours. More theoretical information about this control strategy can be found in Jubany et al. [15].

Fig. 3 shows the inflow profile in this start-up experiment divided into two periods with different level of control strategy implementation. During the first 22 d (period α), the inflow control was done manually. At the beginning, the OUR in R3 was mainly due to endogenous decay of heterotrophs which were predominant. Moreover, this value was almost equal to the maximum OUR due to nitrite consumption. This reason made it impossible to initialize the automatic control until the 22nd day (period β). Firstly, the automatic control was implemented without automatic inflow increases to test the behavior of the pure on–off controller. In practice, the *off position* was not zero but a minimum value (2.4 L d^{-1}) because of experimental restrictions. From day 22–31 the inflow was manually increased every time that the *on position* remained unchanged for several hours. On day 31 (indicated with a dotted line in Fig. 3), complete on–off control strategy with automatic inflow increases was activated. Fig. 3 also shows three long stops (inflow = 0 L d^{-1} during more than 10 h) which occurred on days 30, 31 and 33 due to experimental problems. The effectiveness of the automatic controller was clearly seen since the inflow was quickly increased reaching values of 40 L d^{-1}. Inflow profile in period β was similar to the results obtained in a previous work where the on–off controller was simulated and optimized and the inflow increased up to 40 L d^{-1} after 20 d of simulated operation [15].

Fig. 3 also shows the concentration of the nitrogenous compounds and the OUR profile in each reactor during the whole experiment. TNN sporadically accumulated during the manual period α. TAN was totally consumed in R2 unlike TNN which built up in R1 and R2. It was probably due to the slower growing rate of NOB than AOB and the presence of some FA in R1 that could inhibit NOB population (from day 22 onward). TNN in R3 (and thus in the effluent of the pilot plant) was higher than the nitrogen concentration allowed (10 mg N L^{-1}). It was a result of the OUR_{sp} tuning that was done during the experiment. In practice, OUR_{sp} value must be between the endogenous OUR (OUR_{end}) and the maximum OUR due to nitratation (OUR_{NOB}^{max}). Fig. 4a shows a simulated OUR profile of a TAN pulse in one reactor in batch mode. Under the existing operation conditions, ammonium is firstly depleted and then nitrite is totally consumed. This figure clearly shows that OUR_{sp} must be fixed at a value lower than OUR_{NOB}^{max}, and higher than OUR_{end} to guarantee no TAN and very low TNN in the effluent. In practice, OUR_{sp} were very low (around 10^{-3} mg O_2 L^{-1} s^{-1}), close to the minimum OUR experimentally determinable.

OUR_{sp} in the controlled period of the start-up II can be seen in Fig. 4b, together with the experimental OUR profile in R3. On day 22, the set point was fixed at a very low value. Later, it was increased because TAN + TNN in the effluent were very low (see Fig. 3) indicating that higher NLR_s could be applied. This new set point was calculated with reference to OUR measurements in R1 and R2 (Eq. (12)). Several values for parameter k were tested and for low values ($k = 4$) TNN accumulation was produced (see Fig. 3 for TNN build-up in R3) while for high values ($k = 6$) the increase of the applied NLR was slow.

$$\text{OUR set point} = \frac{\max(\text{averaged OUR}_{R1}; \text{averaged OUR}_{R2})}{k} \quad (12)$$

Fig. 5 shows the evolution of VSS concentration, SVI and NLR_s along the experiment. Biomass concentration decreased until the automatic inflow control was activated. At the end of the experiment the biomass concentration was around 1800 mg VSS L^{-1} and the VSS/TSS ratio was 0.62. SVI decreased indicating the improvement of the settling characteristics of the sludge but the TSS in the effluent increased from 50 to 150 mg TSS L^{-1} probably due to the more disperse growth. NLR_s was calculated with averaged values (last 6 h) of the inflow to soften the fluctuating behavior. It can clearly be observed that NLR_s was quickly increased when the automatic control was activated. It reached values of 0.8 g N g^{-1} VSS d^{-1} when the OUR_{sp} was the highest and stabilized around 0.4 g N g^{-1} VSS d^{-1} at the end of the experiment.

3.3. Experimental start-up with automatic PI control (start-up III)

The pilot plant was inoculated for the third time with sludge from the WWTP of Manresa (Barcelona). Operational conditions for start-up III are described in Table 5. TAN and COD concentrations in the influent were 2800 mg N L^{-1} and 100 mg COD L^{-1}, respectively. COD concentration was changed to 300 mg COD L^{-1} on day 42 in order to improve the settling characteristics of the sludge [23].

At the beginning, the pilot plant was fed with a NLR_s of 0.05 g N g^{-1} VSS L^{-1} (the same NLR_s as in the full-scale WWTP) and a very low OLR (0.002 g COD g^{-1} VSS $d)^{-1}$). After a week of operation, inflow was stopped for 7 d to perform some batch experiments. Later, inflow was changed manually until day 42, when automatic inflow control was activated (see Fig. 6). Temperature was very low at the beginning (winter time) and soon the heater system in R2 was activated. The lack of temperature control in R1 and R3 was the responsible for the different temperatures

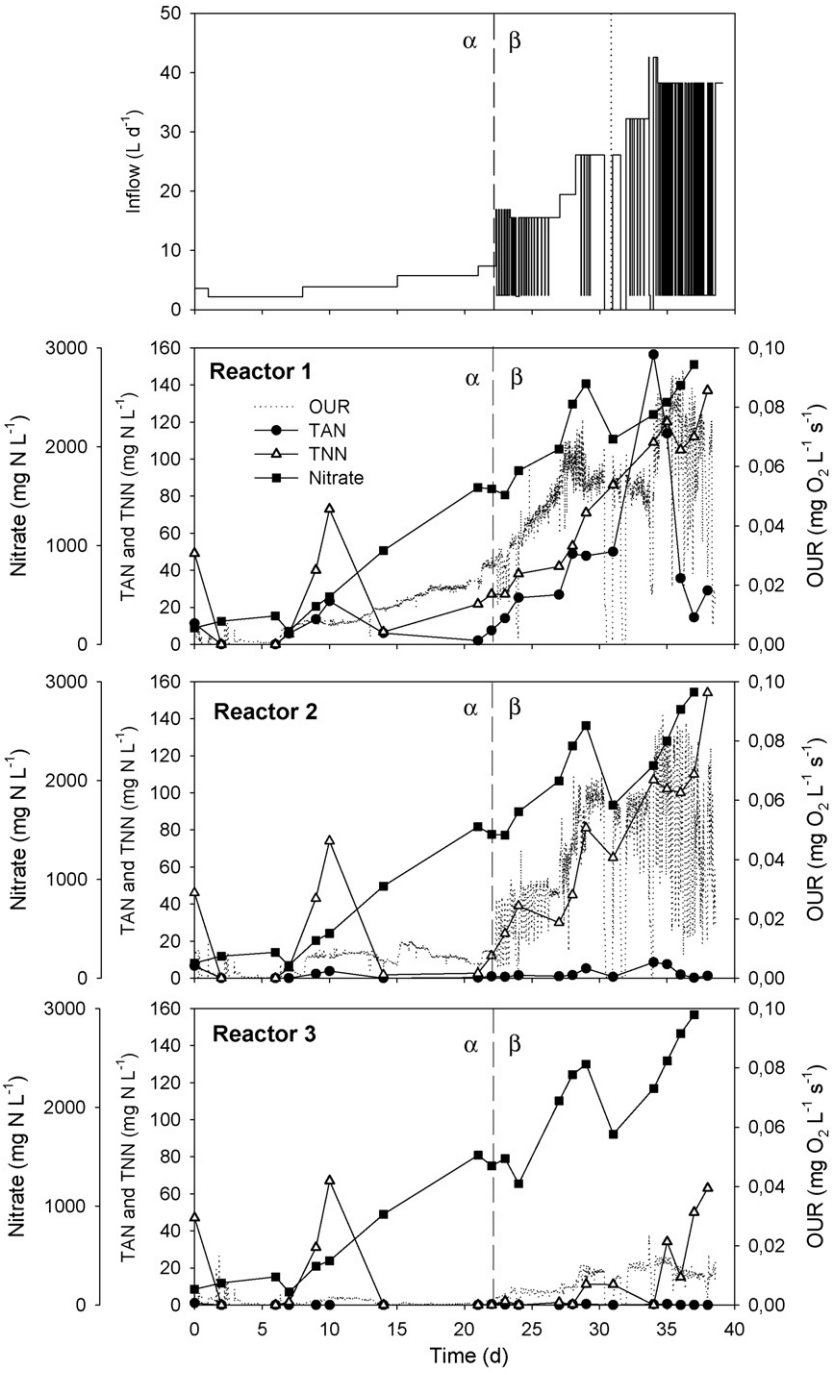

Fig. 3. Inflow pilot plant, nitrogenous compounds and OUR profiles in each reactor during start-up II. (Period α: manual inflow increases; period β: automatic inflow control. Dotted line in period β indicates the beginning of automatic inflow increases).

among reactors. Temperature set point in the controlled reactor was slowly increased to avoid temperatures below 20 °C in the whole system. The low temperature, together with the fact that the inoculated sludge could contain low amount of nitrifying bacteria, provoked that the automatic inflow control could only be activated after 35 d of low NLR_s operation (day 42 if the 7 d of batch experiments are included) compared to the 22 d in start-up II.

Fig. 6 also shows the results obtained in start-up III with respect to nitrogenous compounds and OUR. In period α (manual inflow control), some TAN and TNN accumulated because the applied NLR_s was transitorily higher than the nitrifying capacity of the system. In period β (automatic inflow control), TAN and TNN concentrations behaved similarly than in start-up II and no TAN or TNN accumulation was observed. TAN was totally depleted in R2 and TNN built up in R1 and R2 but it was almost entirely consumed in R3. In order to avoid high TNN concentrations in the effluent, the OUR_{sp} fixed on day 42 (1.4×10^{-3} mg O_2 L^{-1} s^{-1}) was used until the end. In this experiment, low TNN was preferred to variable OUR_{sp}, which could had sped up the start-up but it could also had caused TNN accumulation in R3. OUR profiles shown in Fig. 6 are similar to the ones in Fig.3 except for the oscillatory behavior of the on–off controller previously described.

Biomass also decreased with the manual inflow control (period α) and increased again when the automatic controller was activated

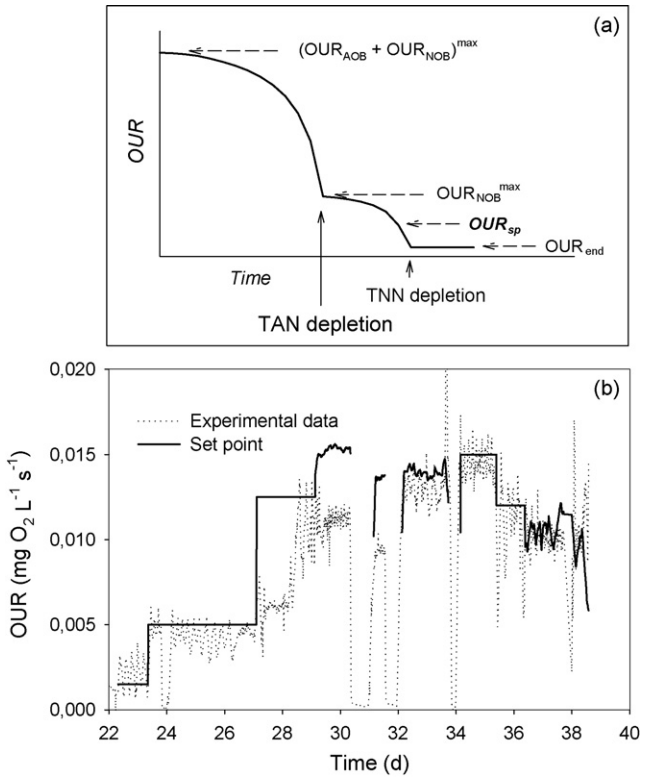

Fig. 4. (a) Theoretical OUR profile of a batch ammonium pulse. Optimal OUR_{sp} compared to maximum OUR values when there is ammonium and/or nitrite in the bulk liquid. (b) OUR profile and OUR_{sp} in R3 during period β (automatic inflow control) of start-up II.

(period β) (see Fig. 7). Biomass concentration was 1300 mg VSS L^{-1} at the end of period β and the VSS/TSS ratio was around 0.70 in the whole experiment. Biomass settling characteristics changed with time: SVI decreased from 86 to 37 mL g^{-1} but TSS in the effluent of the settler increased from 40 to 200 mg TSS L^{-1} indicating disperse growth.

Fig. 7 also shows the NLR_s profile. The fast NLR_s increase during the first days of the automatically controlled period indicated that the controller forced the system to work at its maximum capacity. After these days, the NLR_s continued to increase but with a slower rate. The maximum nitrification capacity of this system turned out to be around 0.5–0.6 g N g^{-1} VSS d^{-1}.

FISH analysis was performed with samples taken on days 0 (beginning of the start-up III), 42 (automatic control activation) and 63 (end of the experiment). Obtained biomass fractions are depicted in Fig. 8. AOB was detected with probe Nso190 whereas with respect to NOB, only *Nitrobacter* species were detected (probe NIT3) while no organisms from the genus *Nitrospira* was identified (probe Ntspa 662 gave negative results). Some researchers found that both populations coexisted in biofilm and activated sludge systems [24] whereas others could only detect one of them [25,26].

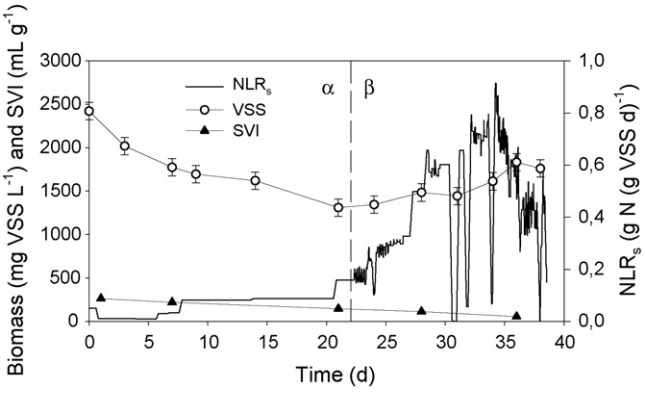

Fig. 5. VSS, SVI and averaged NLR_s during start-up II (Period α: manual inflow increases; period β: automatic inflow control).

FISH results clearly indicated that both AOB and NOB populations increased and that AOB were more abundant than NOB. Supplementary Fig. A shows six representative images corresponding to the three samples analyzed and the two specific probes that gave positive results. At the beginning of the experiment, AOB and NOB fractions were lower than 1%, which demonstrates the difficulty of starting up a nitrifying system with activated sludge from municipal WWTPs. However, at the end of the experiment AOB and NOB fractions had increased to 21 and 5%, respectively. The rest was assigned to heterotrophs.

These results demonstrated that the sludge was enriched in nitrifying bacteria. The higher AOB fraction than NOB fraction was in agreement with the higher growth yield of AOB and it was also in agreement with the simulated results obtained in Jubany et al. [15] and with observations made by other researchers [24,26].

3.4. Automatic control strategies comparison

Both designed controllers required an OUR_{sp} value. As depicted in Fig. 4a, this value should be higher than OUR_{end} but lower than OUR_{NOB}^{max}. However, Fig. 4a is only valid for mainly nitrifying systems. This was not the case at the beginning of the start-up experiments because OUR_{end} was higher than OUR_{NOB}^{max}. This is the main drawback of using in-line OUR for control. Nevertheless, after some days of low NLR (22 in start-up II and 35 d in start-up III) heterotrophic biomass had decreased enough to do not interfere in the estimated OUR value and the automatic control could be initialized. On the other hand, a clear advantage of using OUR measurements and to set the OUR_{sp} value between OUR_{end} and OUR_{NOB}^{max} is that TAN and TNN concentrations in the effluent of the system will be always below the desired limits since the half saturation coefficient for TNN is very low. Therefore, the percentage of nitrification will be always close to 100%.

The strategies implemented in start-up II and start-up III were different in terms of the controller and also in terms of the applied OUR_{sp}. In the on–off strategy (start-up II), the OUR_{sp} was being changed by an open loop supervisory control (manual control) taking into account TAN and TNN concentrations in the effluent to increase the set point at the same time as the nitrifying biomass concentration was increasing. OUR in R1 and R2 were taken as a reference of the nitrifying biomass concentration increase (see Eq. (12)). These OUR_{sp} changes were applied both manually and automatically, nevertheless this method did not work well for the whole experiment because nitrite accumulated in R3. As a result, OUR_{sp} was set at a fixed value in the third experiment (start-up III). In this case, although the set point was too much restrictive, it allowed a better performance because TNN never surpassed the fixed limit (10 mg N L^{-1}). In view of these results, the optimal strategy would be to periodically check the OUR profile in order to define the appropriate set point.

Apart from these small differences, both strategies resulted in fast start-ups with similar profiles of biomass concentration, OUR, TAN and TNN. Nitrogenous compounds concentrations in the effluent were lower than in the periods with manual control. It is interesting to point out that the biomass concentration decreased at the beginning of the experiments due to the heterotrophic decay but it increased again when the automatic controllers were activated. There was a decrease of approximately 1200 mg VSS L^{-1}

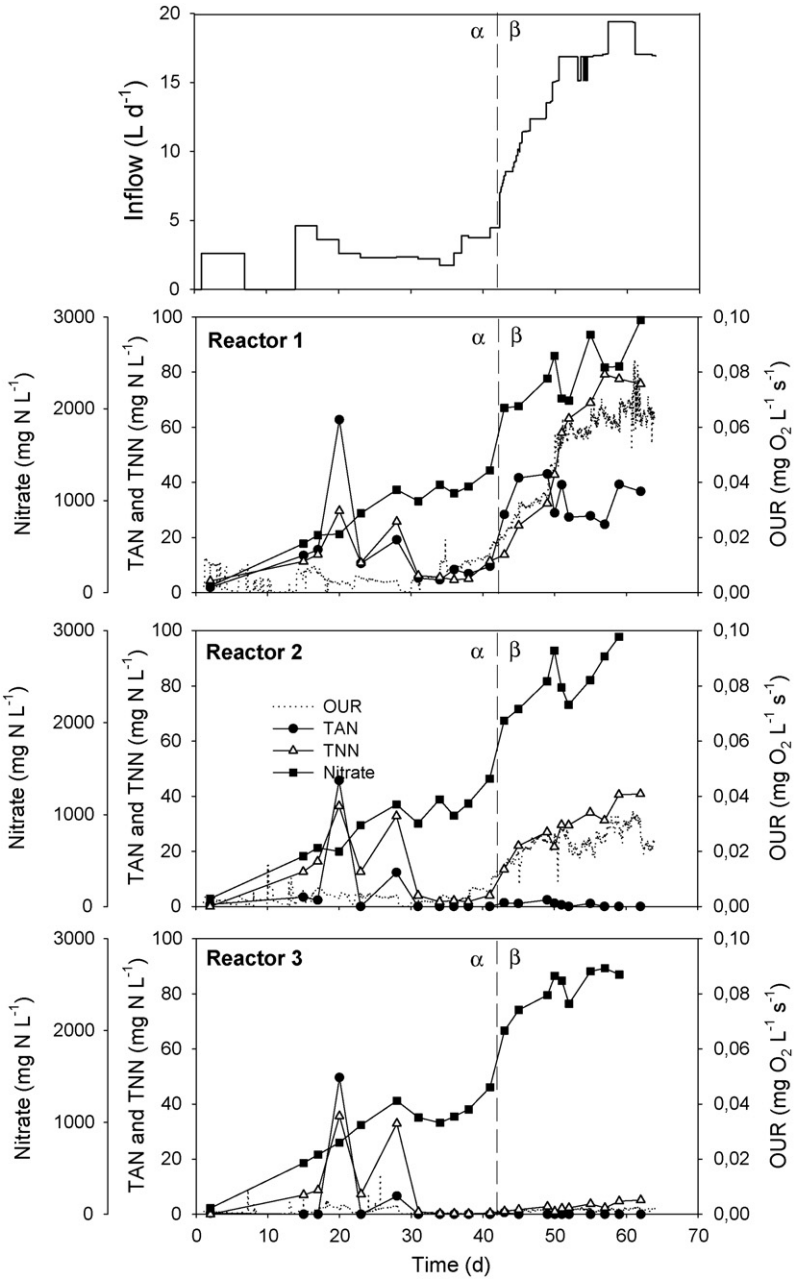

Fig. 6. Inflow pilot plant, nitrogenous compounds and OUR profiles in each reactor during start-up III. (Period α: manual inflow increases; period β: automatic inflow control).

and a following increase of 500 mg VSS L^{-1}, ending with 1800 and 1300 mg VSS L^{-1} in start-ups II and III, respectively. These results indicate that the biomass concentration must decrease approximately 50% before the automatic control could be activated.

Applied NLR_s profiles were quite similar in both experiments. In start-up II, the automatic control was activated on day 22 and 8 d later (day 30) the target NLR_s (0.4 g N g^{-1} VSS d^{-1}) was obtained and surpassed. With respect to start-up III, the automatic control was activated after 35 d with low NLR_s (day 42) and after 8 d (day 50), the NLR_s was stabilized around 0.5 g N g^{-1} VSS d^{-1}. These time lengths are shorter than the 100 d required in start-up I to reach the same NLR_s. Considering both start-up II and III, the maximum NLR_s achieved without TNN accumulation in the effluent was 0.6 g N g^{-1} VSS d^{-1}. NLR_v in start-up II and III were around 3 times higher than in start-up I due to the higher biomass concentration. These results clearly show that the automatic controllers implemented in the system sped up the start-up and enabled obtaining

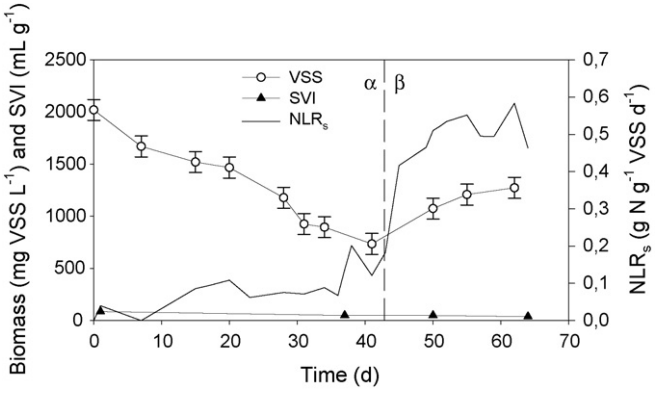

Fig. 7. Biomass concentration, SVI and NLR_s during start-up III (Period α: manual inflow increases; period β: automatic inflow control).

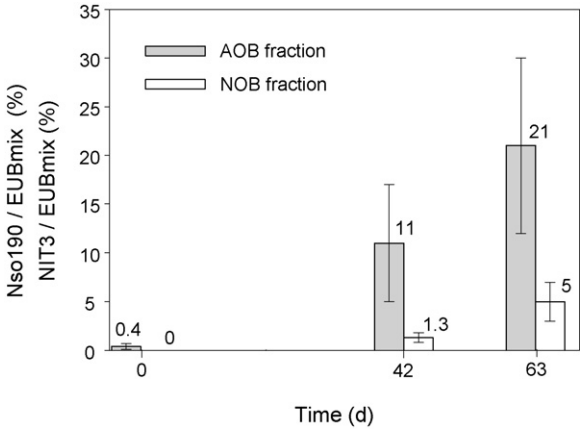

Fig. 8. AOB and NOB fractions in start-up III.

high biomass concentration. The obtained NLR_s is similar to values found in literature but the NLR_v is low when is compared to systems with immobilized biomass or with high SRT due to their higher biomass concentration [5].

3.5. Modelling of the experimental start-ups

The mathematical model described in Section 2.5 was used to simulate the experimental results of the automatic start-ups (II and III). Temperature profiles were introduced in the simulations in order to calculate the temperature-dependent parameters every instant (like maximum specific growth rates, decay rates, inhibition coefficients, etc.). Experimental pH and DO were controlled or were stable in each reactor and thus, considered constant and equal to the experimental values.

Firstly, the model prediction of TNN, TAN and nitrate for the same inflow patterns than in the experimental results of both start-ups was studied. The inflow profile was an input variable for the model and thus, the control loop was not simulated. Initial concentrations of particulate compounds for both start-ups were set to 1% of AOB (X_A), 0.44% of NOB (X_N) (estimated from X_A and the Y_N/Y_A ratio) and 10% of particulate inert products (X_P). The rest of VSS were considered heterotrophs (X_H).

Fig. 9 shows TAN, TNN and nitrate experimental data and model prediction for both start-ups (from 22nd to 40th day for start-up II and from 34th to 64th day for start-up III). All the model concentrations agreed well with the measured concentrations in R1. TAN and nitrate prediction also agreed properly with experimental data in R2 and R3, but TNN concentration was lower in the simulation than the experimental data. The differences between the experimental data for TNN and model predictions could be due to some NOB inhibition that was not predicted by this model.

Fig. 10 shows the experimental data and the model prediction for total biomass concentration in the same periods. The simulations described correctly the general trend of the total biomass concentration. This is one of the most important achievements of this model because there are some works that model successfully similar systems [27–29] but neither of them validate the behav-

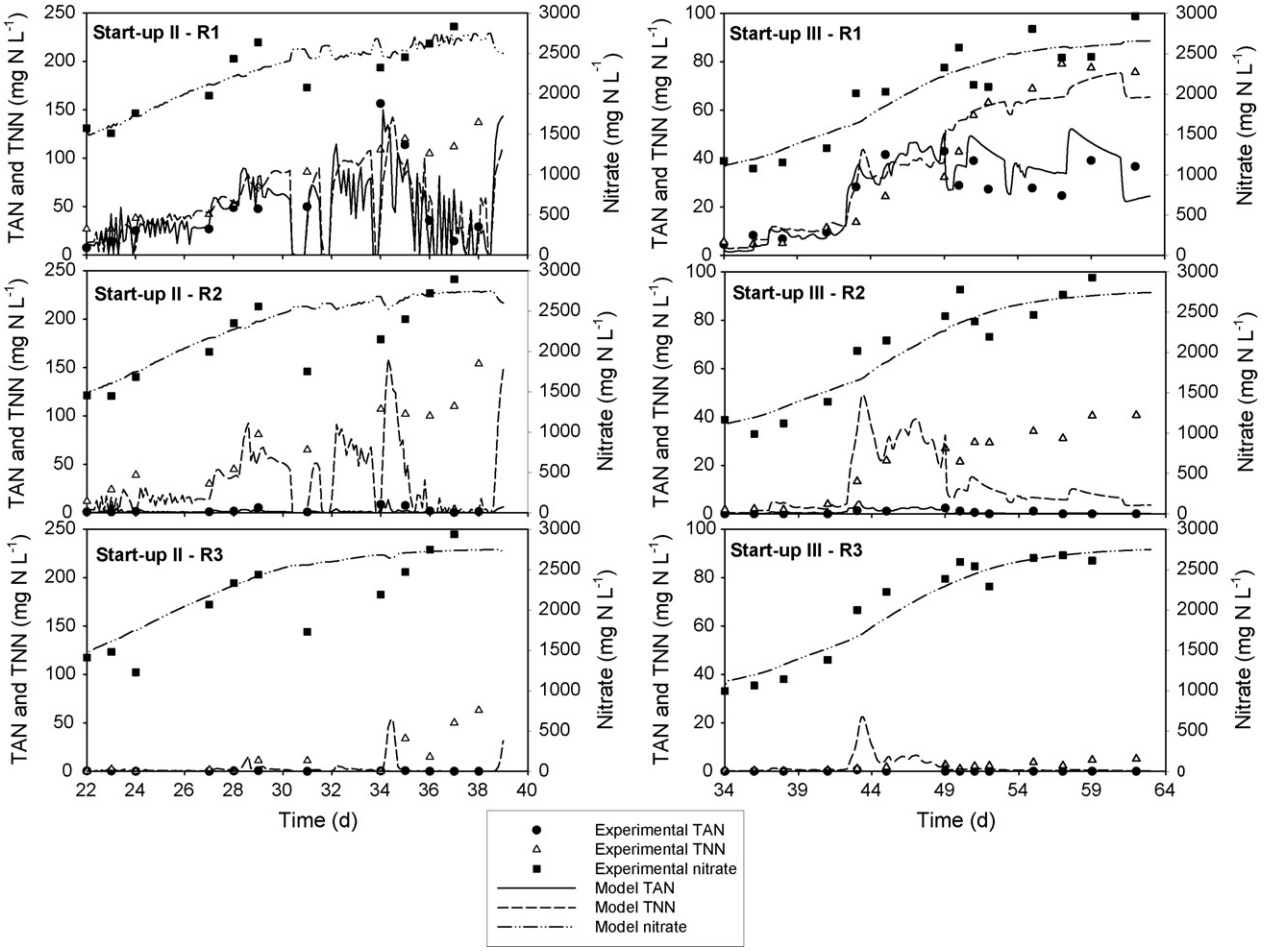

Fig. 9. Experimental data and model prediction of nitrogenous compounds concentrations. Left, start-up II; right, start-up III.

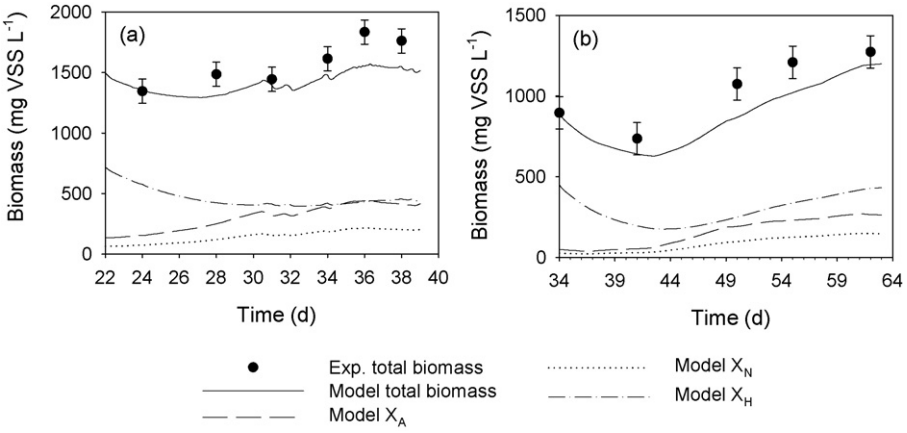

Fig. 10. Experimental data and model prediction of biomass. (a) Start-up II and (b) start-up III.

ior of the biomass concentration comparing with experimental data from pilot plant operation. Fig. 10 also shows the AOB, NOB and heterotrophic biomass concentration profiles predicted by the simulation. In start-up II, AOB and NOB were growing continuously while heterotrophic biomass concentration was decreasing and thus, the sludge was being enriched in nitrifying bacteria. In start-up III, heterotrophs were always more abundant than AOB or NOB because the COD in the influent was higher (300 mg COD L^{-1}) than in start-up II (100 mg COD L^{-1}).

All the results obtained in the simulations using a fixed inflow pattern demonstrated that this model is useful to describe a nitrifying activated sludge treating a high-strength

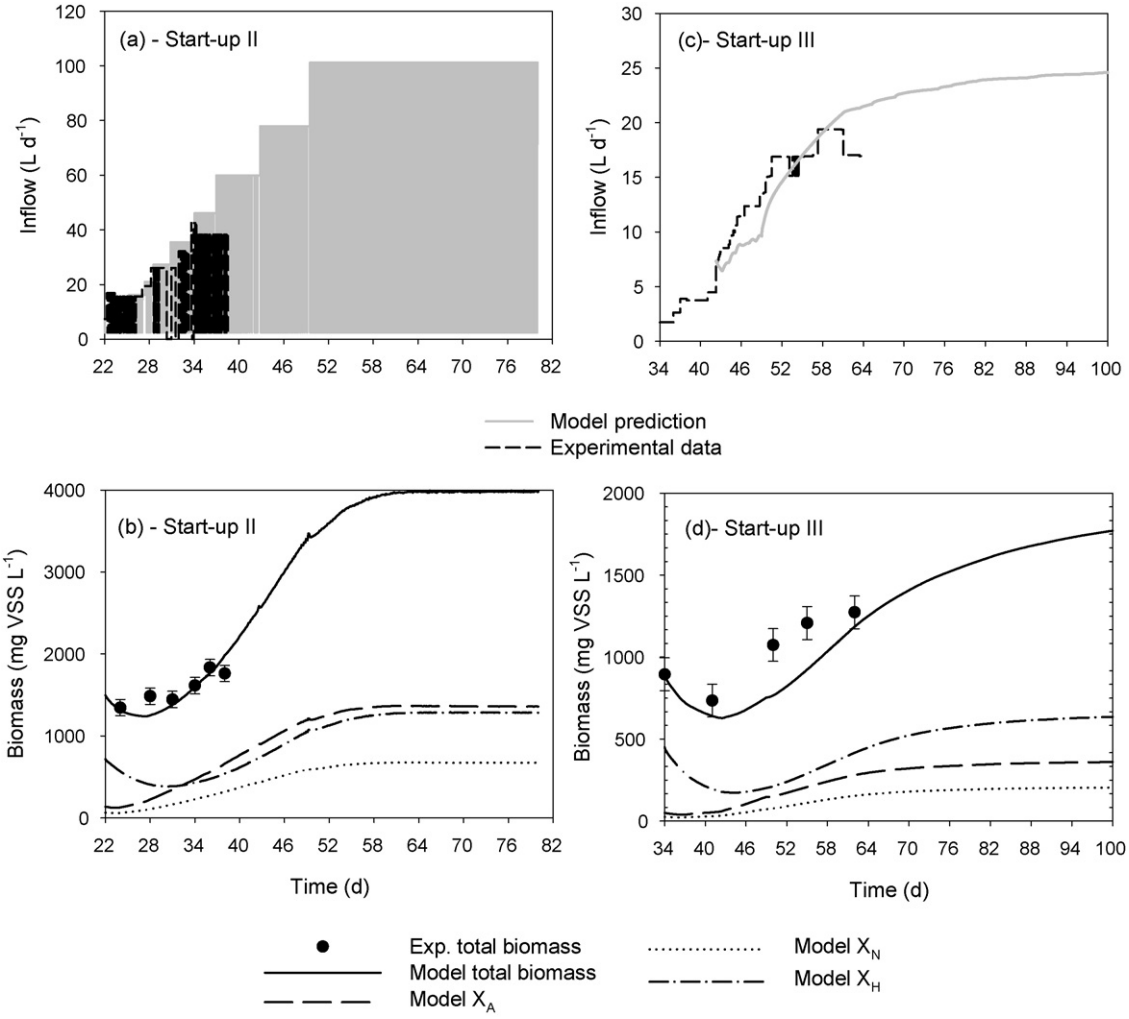

Fig. 11. Left, experimental data (day 22–38) and model prediction in the start-up II simulation (on–off control). (a) Inflow, (b) total biomass, X_A, X_N and X_H. Right, experimental data (day 34–62) and model prediction in the start-up III simulation (PI control), (c) inflow and (d) total biomass, X_A, X_N and X_H.

ammonium wastewater under inhibitory and non-steady state conditions.

After the validation, the model was used to simulate the behavior of the inflow control loops in the long term. In this case, the control loop was included in the model and the control action (inflow value) was calculated by the model with the same frequency than in the experiments. The behavior of both on–off and PI controllers was accurately predicted as shown in Fig. 11.

Furthermore, this model was used to predict the steady state conditions for each different control strategy. The obtained steady states were different in terms of biomass concentration and NLR_s (Fig. 11). In start-up II the predicted biomass concentration was 4000 mg VSS L^{-1} and the NLR_s was 0.823 mg N g^{-1} VSS d^{-1} and in start-up III they were 1770 mg VSS L^{-1} and 0.53 mg N g^{-1} VSS d^{-1}, respectively. These disagreements can be explained with the use of different OUR_{sp} because similar biomass concentration and inflow values than in start-up II simulation were obtained when variable OUR_{sp} (Eq. (12) with $k = 6$) was simulated in start-up III (data not shown). Although the biomass concentration predicted for start-up II (4000 mg VSS d^{-1}) seems quite high compared with the experimental biomass concentration reached in these experiments, this biomass concentration was experimentally obtained in similar conditions in other work [5]. Additionally, these steady states indicate the maxima NLR_ss that could be reached with this configuration and these operational conditions (T, pH, DO, SRT, OUR_{sp}) if no operational problems occurred. Fig. 11 also shows AOB, NOB and heterotrophs concentrations predicted by the model.

The fact that start-up III was low-loaded can be demonstrated if TAN, TNN and nitrate concentrations predicted for both experiments are compared [14]. TAN and TNN accumulation in R1 and R2 were lower in start-up III than in start-up II simulation. Furthermore, these accumulations and the predicted OUR in start-up III tended to decrease with time. This would have been avoided with OUR_{sp} changing according to biomass growth. OUR values in all reactors were also lower than in start-up II simulation due to lower biomass concentration. This fact corroborates the importance of the chosen OUR_{sp} in this kind of controllers.

4. Conclusions

Two automatic control strategies were implemented to speed up the start-up of a completely nitrifying system treating high ammonium concentration when the sludge from municipal WWTP was used as inoculum: an on–off controller with successive inflow increases and a PI controller. These control loops were based on OUR as controlled variable and the inflow as manipulated variable.

The start-up time was decreased from 100 d in the manual start-up experiment to 30–40 d in the experiments with automatic control, while the maximum NLR_s achieved was increased from 0.4 to 0.6 g N g^{-1} VSS d^{-1} with automatic control. Experimental start-ups with both controllers led to similar results in terms of TAN, TNN and VSS concentration, and OUR profiles. The 3-reactor configuration with OUR controlled in the third reactor allowed a fast and reliable start-up with low TAN and TNN concentration in the effluent (TAN + TNN < 10 mg N L^{-1}) and non-limiting substrate concentration in the first two reactors.

The required equipment for the OUR measurement is cheaper, needs less maintenance and is more easily available than TAN and TNN measurements. The OUR_{sp} is the more sensible parameter of the controller. When OUR_{sp} of the controllers is set between OUR_{NOB}^{max} and OUR_{end}, an effluent with very low TAN and TNN concentration is obtained. A faster start-up is possible choosing an OUR_{sp} closer to OUR_{NOB}^{max} although a higher possibility for TNN accumulation exists.

The simulation of both control strategies described quite well the experimental data (including the total biomass concentration) and was further used to predict the steady state conditions. It was confirmed that the OUR_{sp} value is of great importance in the final biomass concentration. For an optimal operation (maximum NLR_s), the OUR_{sp} should be changed according to the biomass concentration in the system.

Acknowledgements

This work has been supported by the European Commission (REMOVALS project, Contract FP6-018525). The authors are members of the GENOCOV group (Grup de Recerca Consolidat de la Generalitat de Catalunya, SGR05-00721). Irene Jubany received a predoctoral fellowship from the Ministerio de Educación y Ciencia (Spanish Government). The authors would like to thank the Microscopy Service of the Universitat Autònoma de Barcelona for its technical assistance with confocal microscopy.

Appendix A. Supplementary data

Supplementary data associated with this article can be found, in the online version, at doi:10.1016/j.cej.2008.02.010.

References

[1] S. van Hulle, S. Van Den Broeck, J. Maertens, K. Villez, B. Donckels, G. Schelstraete, E. Volcke, P. Vanrolleghem, Construction, start-up and operation of a continuously aerated laboratory-scale SHARON reactor in view of coupling with an Anammox reactor, Water SA 31 (2005) 327–334.
[2] S. Chen, C. Chen, Y. Shen, C. Chiu, H.H.J. Cheng, Treatment of high-strength nitrate wastewater by biological methods—operational characteristics study, Water Sci. Technol. 34 (1–2) (1996) 269–276.
[3] W. Verstraete, H. Vanstaen, J.J.P. Voets, Adaptation to nitrification of activated sludge systems treating highly nitrogenous waters, J. Water Pollut. Control Fed. 49 (1977) 1604–1608.
[4] M. Vallés-Morales, J. Mendoza-Roca, A. Bes-Pia, A. Iborra-Clar, Nitrogen removal from sludge water with SBR process: start-up of a full-scale plant in the municipal wastewater treatment plant at Ingolstadt, Germany, Water Sci. Technol. 50 (10) (2004) 51–58.
[5] J. Carrera, J.A. Baeza, T. Vicent, J. Lafuente, Biological nitrogen removal of high-strength ammonium industrial wastewater with two-sludge system, Water Res. 37 (2003) 4211–4221.
[6] A. Galí, J. Dosta, S. Mace, J. Mata-Alvarez, Start-up of a biological sequencing batch reactor to treat supernatant from anaerobic sludge digester, Environ. Technol. 27 (2006) 891–899.
[7] W. Ghyoot, S. Vandaele, W. Verstraete, Nitrogen removal from sludge reject water with a membrane-assisted bioreactor, Water Res. 33 (1999) 23–32.
[8] J. Campos, J. Garrido-Fernández, R. Méndez, J. Lema, Nitrification at high ammonia loading rates in an activated sludge unit, Bioresour. Technol. 68 (1999) 141–148.
[9] J. Suescun, X. Ostolaza, M. Garcia-Sanz, E. Ayesa, Real-time control strategies for predenitrification—nitrification activated sludge plants biodegradation control, Water Sci. Technol. 43 (2001) 209–216.
[10] J.A. Baeza, D. Gabriel, J. Lafuente, Improving the nitrogen removal efficiency of an A2/O based WWTP by using an on-line knowledge based expert system, Water Res. 36 (2002) 2109–2123.
[11] M. Casellas, C. Dagot, M. Baudu, Set up and assessment of a control strategy in a SBR in order to enhance nitrogen and phosphorus removal, Process Biochem. 41 (2006) 1994–2001.
[12] S. Marsili-Libelli, Control of SBR switching by fuzzy pattern recognition, Water Res. 40 (2006) 1095–1107.
[13] I. Jubany, J.A. Baeza, J. Carrera, J. Lafuente, Respirometric calibration and validation of a biological nitrite oxidation model including biomass growth and substrate inhibition, Water Res. 39 (2005) 4574–4584.
[14] I. Jubany, Operation, modelling and automatic control of complete and partial nitrification of highly concentrated ammonium wastewater, Ph.D. Thesis, Universitat Autònoma de Barcelona, Barcelona, Spain, 2007, ISBN: 978-84-690-7378-0 (http://www.tesisenxarxa.net/TESIS_UAB/AVAILABLE/TDX-1005107-170622//ijg1de1.pdf).
[15] I. Jubany, J.A. Baeza, J. Carrera, J. Lafuente, Model-based design of a control strategy for optimal start-up of a high-strength nitrification system, Environ. Technol. 28 (2007) 185–194.
[16] J. Baeza, D. Gabriel, J. Lafuente, An expert supervisory system for a pilot WWTP, Environ. Modell. Softw. 14 (1999) 383–390.
[17] APHA, Standard methods for the examination of water and wastewater, 19th ed, American Publishers Health Association, Washington, DC, USA, 1995.

[18] S. Wyffels, S. van Hulle, P. Boeckx, E. Volcke, O. van Cleemput, P. Vanrolleghem, W. Verstraete, Modeling and simulation of oxygen-limited partial nitritation in a membrane-assisted bioreactor (MBR), Biotechnol. Bioeng. 86 (2004) 531–542.
[19] V. Vadivelu, Z. Yuan, C. Fux, J. Keller, Stoichiometric and kinetic characterisation of Nitrobacter in mixed culture by decoupling the growth and energy generation processes, Biotechnol. Bioeng. 94 (2006) 1176–1188.
[20] A. Anthonisen, R. Loehr, T. Prakasan, E. Srineth, Inhibition of nitrification by ammonia and nitrous acid, J. Water Pollut. Control Fed. 48 (1976) 835–852.
[21] M. Henze, W. Gujer, T. Mino, M. van Loosdrecht, Activated Sludge Models ASM1, ASM2, ASM2d, ASM3, IWA Publishing, London, 2000.
[22] MATLAB, User's Guide, Version 6.5 (Release 13), T. Mathworks (Ed.), Natick, USA, 2002.
[23] F. Çeçen, E. Orak, Nitrification of fertilizer wastewaters in a biofilm reactor, J. Chem. Technol. Biotechnol. 65 (1996) 229–238.
[24] C. Mota, J. Ridenoure, J. Cheng, F. De Los Reyes, High levels of nitrifying bacteria in intermittently aerated reactors treating high ammonia wastewater, FEMS Microbiol. Ecol. 54 (2005) 391–400.
[25] K. Egli, C. Langer, H. Siegrist, A. Zehnder, M. Wagner, J.J.R. van der Meer, Community analysis of ammonia and nitrite oxidizers during start-up of nitritation reactors, Appl. Environ. Microbiol. 69 (2003) 3213–3222.
[26] S. Tsuneda, T. Nagano, T. Hoshino, Y. Ejiri, N. Noda, A. Hirata, Characterization of nitrifying granules produced in an aerobic upflow fluidized bed reactor, Water Res. 37 (2003) 4965–4973.
[27] J. Dosta, A. Galí, E. Benabdallah, S. Macé, J. Mata-Álvarez, Operation and model description of a sequencing batch reactor treating reject water for biological nitrogen removal via nitrite, Bioresour. Technol. 98 (2007) 2065–2075.
[28] V. Pambrun, E. Paul, M. Spérandio, Control and modelling of partial nitrification of effluents with high ammonia concentrations in sequencing batch reactor, Chem. Eng. Process. 47 (2008) 323–329.
[29] S. van Hulle, E. Volcke, J. López Teruel, B. Donckels, M.C.M. van Loosdrecht, P. Vanrolleghem, Influence of temperature and pH on the kinetics of the Sharon nitritation process, J. Chem. Technol. Biotechnol. 82 (2007) 471–480.